



Research Paper

Synthesis, properties and mechanism of the ion exchange resins based on 2-methyl-5-vinylpyridine and divinylbenzene in the catalytic disproportionation of trichlorosilane



Andrey V. Vorotyntsev^{a,*}, Anton N. Petukhov^a, Dmitriy A. Makarov^a, Evgeny N. Razov^b, Ilya V. Vorotyntsev^a, Alexander V. Nyuchev^c, Natalia I. Kirillova^c, Vladimir M. Vorotyntsev^a

^a Nizhny Novgorod State Technical University n.a. R.E. Alekseev, Nanotechnology and Biotechnology Department, Laboratory of Membrane and Catalytic Processes, Nizhny Novgorod, 603950, Russian Federation

^b Institute for Problems in Mechanical Engineering, Russian Academy of Sciences, Nizhny Novgorod, 603024, Russian Federation

^c N.I. Lobachevsky State University of Nizhny Novgorod, Nizhny Novgorod, 603950, Russian Federation

ARTICLE INFO

Keywords:

Heterogeneous catalysis
Suspension polymerization
The ion exchange resin
Trichlorosilane
Catalytic disproportionation
Silane
Silicon

ABSTRACT

The variety of catalysts based on macroporous ion exchange resins using 2-methyl-5-vinylpyridine cross-linked with divinylbenzene (2M5VP/DVB) was investigated in the disproportionation of trichlorosilane (TCS) in a continuous-flow reactor. The effects of the reaction temperature and surface area on TCS disproportionation kinetics was investigated using three types of catalysts based on 2M5VP/DVB with a different pore ratios (toluene(tol)/heptane(hep)) and in the temperature range of 333.2 K and 453.2 K. The results indicate that within this range, the higher reaction temperatures result in an increase in the conversion rate to TCS at equilibrium. The effects on the specific catalyst surfaces were determined and the catalyst (2M5VP/DVB-hep/tol) with the highest specific surface area exhibited better catalytic activity. Variable temperature studies on the catalytic activity of 2M5VP/DVB-hep/tol revealed an activation energy of $24.06 \pm 0.72 \text{ kJ mol}^{-1}$ for 2M5VP-hep/tol and $34.30 \pm 1.03 \text{ kJ mol}^{-1}$ for Amberlyst A-21 resins. TCS disproportionation was investigated using a non-stationary process and showed the desorption of STC from the active sites of the catalyst to be the rate determining step. Using FTIR analysis, we have already established that the resin after exposure to HCl or TCS undergoes protonation of the nitrogen atom in the pyridine ring with intermediate formation of $\text{N}^+ \text{H} \cdots \text{Cl}^-$ / $\text{N}^+ \text{H} \cdots \text{SiCl}_3^-$. Based on the reaction data obtained in this study, a probable mechanism of the reaction has been proposed.

1. Introduction

Widespread industrial development is leading to increased energy demand, requiring an increase in the production capacity and the processing of organic and non-environmentally-friendly energy sources. Consequently, it is imperative to search for alternative, environmentally-friendly, or renewable energy sources. The primary "green" source is solar energy as an environmentally compatible and inexhaustible source of energy [1–3]. To these ends, one of the major feedstocks for the production of photovoltaic components is the polycrystalline silicon [4–10]. At present, the main process used to obtain polycrystalline silicon is the Siemens-process [11–15], which is used by more than 80% of the polysilicon manufacturers in the world. Nevertheless, this process has several disadvantages, such as high capital

investment, high energy consumption costs, and difficulties in the preparation of electronic-grade polysilicon products.

Production of electronic-grade polysilicon (9N) by thermal decomposition of silane (SiH_4) is attracting greater interest, as it has lower investment and low energy consumption costs, with minimal environmental pollution in production [7,16,17]. In addition, silane has wide applications in opto-electronics, micro- and nano-electronics for use in solar cells, and the semiconductor industry [4–6].

Currently, silane is mainly produced by the catalytic disproportionation of trichlorosilane [18–25], decomposition of magnesium silicide [7] and variations thereof [26–30], and plasma treatment [31–35]. The method of the TCS disproportionation involves a simple process with a lower cost and high industrial safety, compared with the method based on the decomposition of magnesium silicide.

* Corresponding author at: Nizhny Novgorod State Technical University n.a. R.E. Alekseev, Nanotechnology and Biotechnology Department, Laboratory of Membrane and Catalytic Processes, Minina str. 24, Nizhny Novgorod, 603950, Russian Federation.

E-mail address: an.vorotyntsev@gmail.com (A.V. Vorotyntsev).

The production of silane by the TCS disproportionation occurs through three major reversible reactions:



The rate of the TCS disproportionation can be increased by catalysis, and several types of catalysts have been used to achieve this such as Lewis acids and acyclic nitriles [36–40]. However, almost all such catalysts introduce various impurities into the products. The usage of organic homogeneous catalysts containing a nitrogen atom as an electron donor pair leads to challenging separations of products from the reaction mixture. Among the variety of organic and inorganic compounds which may catalyze TCS disproportionation, special interest has been paid to an anion exchange resins using chemically-inert matrices with a variety of functional groups and large specific surface areas [41–50].

Currently, the catalyst of choice for TCS catalytic disproportionation derives from ion exchange resins (IER) based on styrene-divinylbenzene (ST/DVB), and modified resins containing strongly basic functional groups ammonium groups in the form of chlorine. The most commonly used process for TCS catalytic disproportionation uses two types, Amberlyst™ A-21 Dry and Amberlite® IRA-400 [42–48]. The main disadvantage of its use is its poor thermal stability, which is limited to 100 °C; hence limiting the possibilities of the kinetic reactions (1)–(3) [51].

In light of these limitation, we have investigated the catalytic activity of thermally-stable resins based on a copolymer of vinylpyridine (VP)-divinylbenzene (DVB) [24,41,44,52,53]. Using VP resins allows for disproportionation of TCS at higher temperatures (100–150 °C), which can lead to increased yield of the disproportionation product, according to thermodynamic calculations [50].

Commercial vinylpyridine resins available from the Vertellus company (Reillex® resins) use processing technology that was developed in Russia [50,52]. Although according to [44,50], they are shown to have a higher catalytic activity in the disproportionation reaction of TCS; however, have not yet been used in the modern processes to produce silane.

The catalytic disproportionation of TCS using resins of different copolymers has been utilized in industrial reactive distillations column and continues to undergo further improvements to this established process such as the use of new catalysts and column design [1,10,29,47,48]. The authors [47,48] conducted detailed theoretical and experimental calculations for the reactive distillation of TCS on Amberlyst™ A-21 using Aspen Plus software package with the base of the NIST. Using the data obtained from these studies [47,48], a modification on the classical scheme of the reactive distillation column and membrane purification [49] has been applied to obtain a silane with the addition of various intermediate sections to the column capacitors to reduce the load on the main capacitor after rectification, leading to a 56% reduction in energy consumption.

Today, one of the greatest scientific challenges is the design of nanomaterials for catalytic technologies which are able to intensify the key technological processes. Knowledge of the nanoscale behavior of materials will be integral in answering otherwise elusive questions and solving a variety of problems such as improving of the existing technologies, increasing the efficiency of the solar energy, and improving the selectivity and activity of catalysts. Greater insight into these factors may also contribute to the design the novel materials which will provide added predictive power of catalyst activity.

Thus, nowadays nanotechnology research and development in the field of catalysis are the most important tasks for the design of novel materials, which will allow to predict the properties of catalysts during their synthesis and selection, that is, to perform high-performance screening for technological processes.

The scientific significance of the creation of functionalized catalysts pursues two goals, important in the fundamental – understanding of the mechanisms of catalytic conversions on known active sites, and in practical – production of stable catalysts with optimal activity, selectivity and reproducibility of properties for specific technological processes. Also, it's important to note the possibility of implementing closed technological cycles (recycling), in connection with the thermal stability AER and their easy regeneration, in comparison with traditional metal catalysts prone to poisoning by catalytic poisons.

The scientific novelty of the tasks is the main world scientific research in this area is reduced to the modernization of the hardware execution of the technological process, as well as the variation in technological parameters (temperature, pressure, flow ratio, etc.) and very rarely capture in the fundamental aspects from the point of view search for new, more productive catalysts and study of kinetic dependencies for establishing the mechanism of reactions. An important feature of this work is that the search for a suitable catalytic system was carried out from the point of view of the reaction mechanism. The choice of trichlorosilane disproportionation as a heterogeneous catalyst was based on the work of Benkezer and Ring, the essence of which consists in the formation of an ion pair of $\text{RNH}^+\text{SiCl}_3^-$ and an intermediate of the type $[\text{RHSi}_2\text{HCl}_6]$ and its decomposition with the formation of final products. The mechanism of the reaction has been studied in detail (in particular, due to some discrepancies in the mechanism of Benkezer and Ring), the reason for the decrease in the yield of the target products due to the reactions of the dismutation and the effect of the limiting stage on the yield of the main products was made.

These results inspire the current study on the catalytic properties of 2M5VP/DVB resins with different physical and chemical parameters in the disproportionation of TCS. For the first time, a study of the adsorption of TCS and STC on our samples has been performed and the limiting stage of desorption of the resin has been established.

2. Experimental

2.1. Materials

2-methyl-5-vinylpyridin (2M5VP) was purchased from ("Chemical Line", Russia) and used after vacuum distillation. The initiator, 2-2'-azobisisobutyronitrile 99% (AIBN) was purchased from ("Chemical Line", Russia) and used without any further purification. The diluents *n*-heptane (hep) and toluene (tol) ("Vekton", Russia), and commercial divinylbenzene 80% (DVB) ("SigmaAldrich", Germany) were used without any further purification. For disproportionation of TCS, the reagents used were: trichlorosilane (99.998%, Firm HORST Ltd., Russia), helium (99,99999%, "Monitoring", Russia) and hydrogen (99.99998%, "Monitoring", Russia).

2.2. Resin synthesis

The 2M5VP/DVB resin was prepared in a 500 ml three-neck round-bottom glass reactor equipped with a mechanical stirrer, reflux condenser and a nitrogen gas inlet tube. First, the aqueous phase (AP) was produced by the addition of a specific amount of gelatin (0.5 wt.% about AP, respectively) and NaCl (2 wt.% about AP). The organic phase (OP) was composed of monomers mixture with various composition diluents (100tol/0 hep, 90tol/10hep or 50tol/50hep at 100% v/v) and AIBN used as initiator (1.0 mol%). OP was added slowly to AP previously prepared under stirring at 40 °C, using an AP/OP ratio of 3/1. The polymerization was performed at 80 °C under constant stirring (400 rpm) for 24 h by using a thermostatic water bath. After the allotted reaction time (8 h), the polymeric beads were washed with water and methanol, filtered, and passed through a series of sieves with a standard mesh size to determine the particle size distribution.

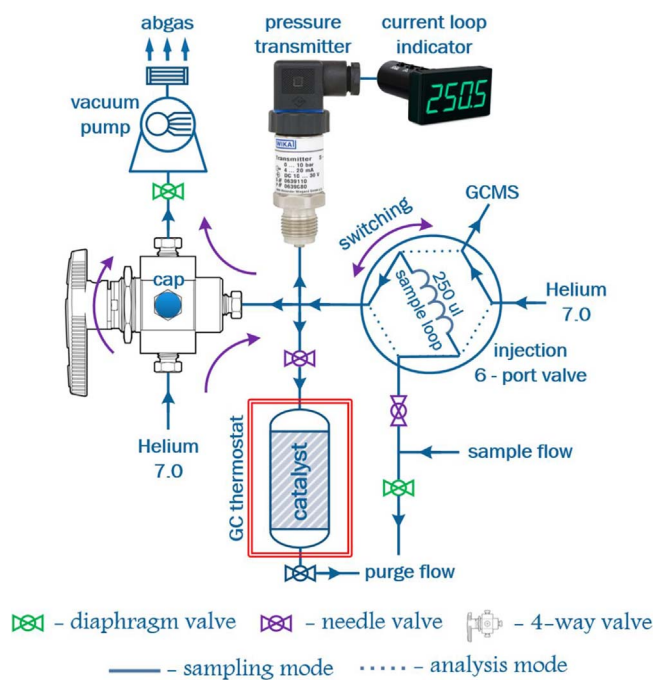


Fig. 1. Apparatus for express-analysis of catalyst.

2.3. Apparatus and procedures for disproportionation TCS

2.3.1. Static method for evaluating catalytic activity

The static method was chosen for determination of the catalytic activity of the catalysts in the disproportionation reaction of TCS. The reaction apparatus was prepared as a mixture of TCS and helium in a thermostatically controlled reactor filled with the catalyst.

The experimental setup is shown in Fig. 1. The catalyst after loading into a 10 cm^3 reactor to study the reaction under static conditions was evacuated with a HiCube Eco 80 turbomolecular pump (Pfeiffer Vacuum, Germany) to 10^{-5} mbar at 353 K for 12 h to free the sample pores. The experiment, under static conditions, was carried out with an excess of the catalyst with respect to trichlorosilane. Before the beginning of the experiment, the system was evacuated and heated up to 353 K using a TCS/He gas mixture in a ratio 1/20. The gas mixture was supplied from a sample flow line injected by a Valco 6-port valve to vacuum sample inlet system with a pressure 10 kPa indicated on the current loop by the pressure transmitter. After that procedure, a gas mixture was supplied to the reactor in the presence of catalyst (catalyst weight 1 g), after which it was cut off from the vacuum system and allowed to set for 1 h at a temperature of 353 K. Then the gas mixture from the reactor was analyzed by GCMS analysis at the moment when steady-state conditions and thermodynamic equilibrium were achieved.

2.3.2. Dynamic method for evaluating catalytic activity and kinetic dependencies

Based on the results of the express-analysis, the catalyst with the highest activity was determined and subsequently studied under dynamic conditions in the setup shown in Fig. 2 to determine the kinetic dependencies. The apparatus used in the reaction experiment (Fig. 2) was made from 316SS stainless steel and various Swagelok ball valves with Dow Corning® Valve Lubricant, resistant to chlorides of silicon and hydrogen chloride.

The vapor phase of the reaction was prepared by passage of the carrier gas through a bubbler filled with TCS (Fig. 2, temperature liquid of TCS was 278 K) in which carrier gas passes through the layer of liquid TCS and saturated with its vapors. The carrier gas flow for each reaction ranged from 10–30 ml/min and allowed for the determination of the kinetic curves. Several parameters can be adjusted to change the

concentration of components in the vapor-gas phase can be changed parameters such as the temperature of the bubbler with TCS, and the flow rate of the carrier gas. We used TCS and helium containing water and oxygen at a level of 0.1 and 0.2 ppm, respectively.

The continuous flow reactor was used for carrying out the catalytic disproportionation of TCS. A stainless steel cylinder with a length of 420 mm and an inner diameter of 10.26 mm with Fitok ferrule union 3/4"-1 1/4" was used in the continuous flow reactor and facilitates the investigation of the catalytic behavior. The reactor design allows for quick assembly and disassembly to examine the catalytic activity of the catalysts. In the experimental research, the reactor temperature varied within the range of 333 K and 423 K. Resins were placed in the reactor, purged with a carrier gas while gradually heating from 298 K to 423 K, then treated with a mixture of TCS in the carrier gas at the desired temperature.

2.3.3. Non-stationary method (impulse chemisorption) determine the limiting stage

To determine impulse chemisorption, a reactor with a 5 m (OD – 3 mm, ID – 2 mm) GC column was installed to a GC thermostat. The column was heated to a temperature of 333–373 K and the sample injected into the carrier gas stream, delivered at a rate of 40 ml/min from 1 to 10 mg TCS at intervals between 1 to 30 min. The gas exiting the column was then analyzed by MS.

2.4. Analysis

2.4.1. Characterization resins

The resins were characterized by a variety of analytical methods. The surface area and porosity were determined by the low-temperature nitrogen adsorption measurements following the BET method by Autosorb iQ C (Quantachrome Instruments, USA) [53]. The procedure of the measurement is described in detail in our previous work [27]. Samples resins were characterized by FTIR spectroscopy by IRRAfinity-1 (Shimadzu, Japan) at ambient temperature and inert atmosphere of argon (99.9995%). Fourier transform infrared spectroscopy was performed on samples prepared as KBr pellets [54]. A minimum of 30 scans was signal-averaged with a resolution of 4 cm^{-1} in the $4000\text{--}400\text{ cm}^{-1}$ range. All other parameters were not controlled and corresponded to the testing characteristics established by the manufacturer. The sample measurements were carried out in the film samples treated in a potassium bromide matrix. Samples for FTIR were prepared by cooperative pressing of resins and dehydrated. KBr powders were pressed at pressure 100 MPa under vacuum at 25 °C. The morphological and visual appearance characteristics were observed by scanning electron microscopy Vega II (Tescan, Czech Republic) at a voltage of 20 kV with a backscattered electron (BSE) detector and a detector of reflected electrons (RE) detector with zooming from 500 to 8000, and 20000. The use of BSE and RE detectors for the acquisition of high contrast images in comparison to the secondary electron (SE) detector. The apparent density was measured by the graduated cylinder method [55]. The ion exchange capacity of the pellicular resins was determined by titration. Following the IUPAC recommendations [56], the resins were converted to the chloride-form (Cl-form) and the ion exchange capacity was determined by titration with a standard aqueous AgNO_3 solution [57].

Thermodesorption analysis for coupled evolved gas-analysis (Direct EGA-MS) measurements was carried out on a temperature-programmable Double-Shot Pyrolyzer EGA/PY-3030D (Frontier Laboratories, Japan) incorporated in CGMS QP-2010Plus (Shimadzu, Japan). The decomposition onset temperature was determined by 3-sigma method, at the time when the characteristic of mass signal became 3 times higher than the background signal, the corresponding temperature was determined. To perform an experiment, a deactivated stainless-steel sample cup was loaded with approximately 100 μg of sample and dropped into a quartz pyrolysis tube. The quartz tube was surrounded by a tubular furnace, which provided uniform heating and maintained

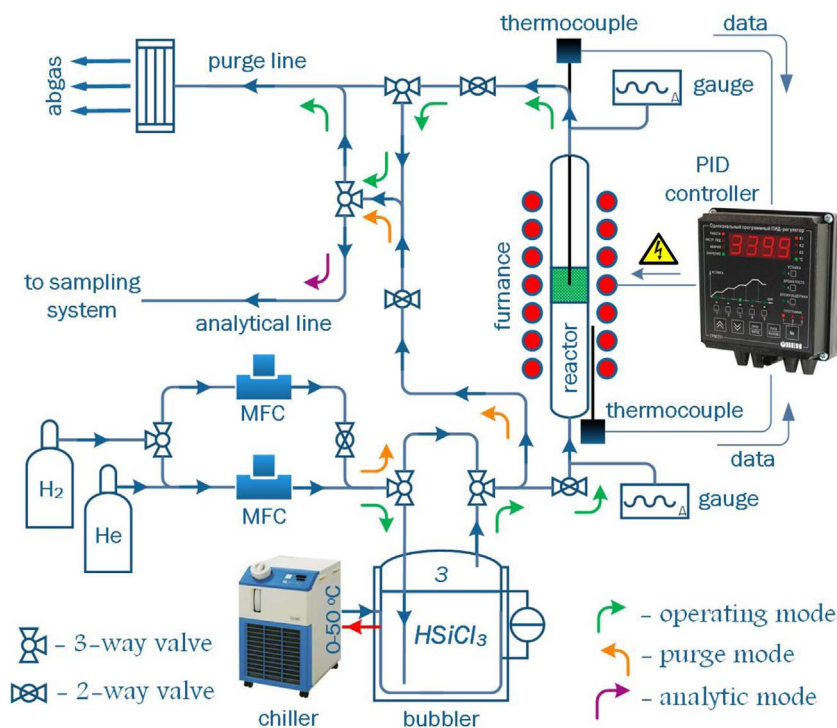


Fig. 2. Apparatus for investigation the disproportionation of TCS.

the pyrolysis temperature in accordance with the following temperature program under a helium flow of 50 ml/min, at the pyrolyzer, and was reduced to 1 ml/min at the capillary column by means of splitter: the 1st stage – holding at 323 K for 10 min, after that, at the 2nd stage the sample was heated in the range of 323–773 K (10 K/min). During the 2nd stage, identification of resulting chromatographic peaks was carried out with the help of a mass selective detector. Ionization in the mass-spectrometer was carried out by electron ionization (EI) at 70 eV and a mass range between 12 and 500 amu scanned at a rate of 2000 s/scan. Reaction products were separated on 2,5 m Tube made of Ultra ALLOY EGA (Frontier Laboratories, Japan) at 373 K (45 min) with the help of selected ion monitoring, carrier gas – helium. Reaction products were identified with the help of NIST-11 database of mass spectra and "GCMS Real Time Analysis" software.

2.4.2. Product analysis

Ex-situ qualitative analysis of the major reaction products was carried out on GCMS – QP2010Plus (Shimadzu, Japan) with a vacuum sample inlet system through an automatic injection valve (Valco Instruments Co Inc, USA). The products which were obtained in the reaction were separated on an Agilent capillary column CP-7434 Select Silanes™ (30 m, film 1,5 μm) with a stationary phase based on trifluoropropylmethylpolysiloxane at 323 K for 10 min; carrier gas – helium. Reaction products were identified with the help of the NIST-11 database of mass spectra and on the basis of the m/z of the formed fragments and «GCMS Real Time Analysis» software.

According to the obtained data the main products consisted from SiH_4 (m/z 30), SiH_3Cl (m/z 64), SiH_2Cl_2 (m/z 99), SiHCl_3 (m/z 133), SiCl_4 (m/z 170).

Fig. 3 shows the chromatogram in total ion current (TIC) mode of the chlorosilanes mixture. It is seen that in the region of 1.7–2.1 min, the decomposition of MCS occurs (due to its high reactivity) with hydrogen chloride formation as a broad peak in the chromatogram, imposing difficulty in accurately determining the concentration of reactants; these challenges are circumvented using SIM (select ion monitoring) mode (Fig. 4). As a result of gas chromatography-mass spectrometry research chromatograms were obtained, mass spectra of chlorosilanes and impurities are shown in the Supplementary

Information (Supplementary Fig. S1-S8).

The quantitative analysis was performed using the absolute calibration method [58] and standard addition. GCMS method provides the detection limits of below 10 ppb and the RSD less than 5% at sub-ppm levels which allows reliable qualification of 99.99999% trichlorosilane on a routine basis as well as control of the process measurement concentrations of main products with mass selective detector.

3. Results and discussion

3.1. Characterization 2M5VP/DVB resins

Porogen is included in the polymerization system as a pore forming agent and plays an important role in the design of the porous microsphere structure [59–61]. In our work, toluene and heptane were selected as the porogen. To investigate the influence of porogen type and amount on the copolymer porous structure, three samples were synthesized at constant monomer concentration.

In the synthesis of 2M5VP/DVB resins (see Table 1), three dilution levels were utilized with the aim of producing different types of porous structures while all other reaction variable remained constant. The porous structure of the copolymer varies considerably depends on the applied porogen type and amount. Large portions of the non-solvating agent, heptane, increases the pore diameter and decreases the specific surface area. By comparison of the external surface and pore size of the prepared microspheres (as shown in Fig. 5), it is noted that the microspheres synthesized with 50% mixture of toluene/heptane as the porogen are more porous than those synthesized with a 90/10 mixture of toluene/heptane or neat toluene. The synthesized resin 2M5VP-hep/tol has similar textural characteristics with the industrial resin Amberlyst A-21, and a smaller specific surface giving rise to a larger exchange capacity. As a result of porosimetry research, isotherms of our samples were obtained and are shown in the Supplementary Information (Supplementary Fig. S9-S11).

The FTIR spectrum of 2M5VP-hep/tol is provided in Fig. 6, the absorption bands at $1635\text{--}1456\text{ cm}^{-1}$ and 820 cm^{-1} are attributed to the symmetric C=N stretching vibration and C–H out-of-plane bending vibration of the pyridine ring in VP chain units, respectively [62],

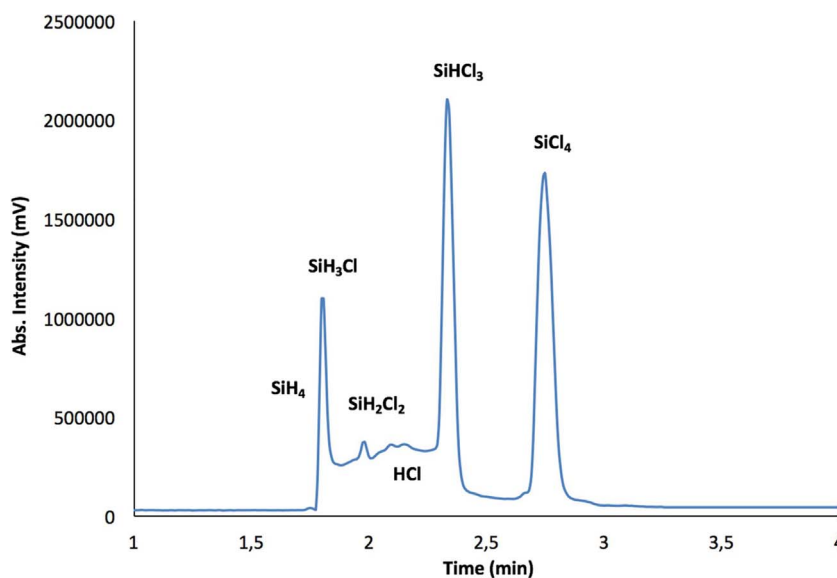


Fig. 3. Chromatogram of the sample mixture of chlorosilanes in TIC mode.

confirming the incorporation of 2M5VP into the copolymer structure.

As seen from Fig. 6 (spectrum 3), when the 2M5VP-hep/tol resin is activated with HCl, a broad band appears in the region of 2600 cm^{-1} , which refers to the $\text{N}^+\text{H}\cdots\text{Cl}^-$ band responsible for the protonation of the nitrogen atom in the pyridine ring.

After exposure of TCS to the resin, its activation occurs and a broad band appears in the region 2600 cm^{-1} . In addition, a new band appears corresponding to the stretching vibration of Si-H at 2250 cm^{-1} , and the TCS bands are absent, likely due to adsorption to the resin.

In the framework of thermal desorption, studies were conducted before the desorption of samples to obtain the characteristic curves of TCS desorption from the surface of the anion exchange resins. The dependences obtained are shown in Fig. 7. The 2M5VP-hep/tol resins undergo an obvious hysteresis in 8 min, likely due to their macroporous structure, wherein the first step occurs by TCS desorption from the surface of the resin, and in the second stage, desorption from the macropores of the resin.

Further, the temperature stability of the samples was determined using thermal desorption analysis, and the results are provided in Fig. 8. It is seen that all the samples are subject to deactivation by thermo-degradation with methyl chloride (m/z 50) formation, and all samples have a similar thermal stability up to 433 K, markedly higher than that

Table 1
Characteristics of 2M5VP resins.

Symbol	Diluents (%v/v, tol/hep)	Specific surface area ($\text{m}^2\text{ g}^{-1}$)	Average pore diameter (nm)	Particle average diameter (μm)	Exchange capacity (meq/g)
2M5VP-tol	100/0	8.0 ± 0.4	31.9 ± 1.6	302	4.5 ± 0.1
2M5VP-tol/hep	90/10	9.0 ± 0.5	32.3 ± 1.6	338	4.8 ± 0.1
2M5VP-hep/tol	50/50	28.2 ± 1.4	80.4 ± 4.0	362	5.3 ± 0.2
Amberlyst A-21 ^a	–	35.0 ± 1.8	11.0 ± 0.6	590	5.0 ± 0.2

^a Industrial grade resin for disproportionation of TCS.

of the industrial grade resin Amberlyst A-21 (Maximum operating temperature 377 K, Product Data Sheet) used in the disproportionation TCS (Fig. 8). This is quite a remarkable fact, given that according to the thermodynamic calculations of Ref. [63], the yield of the desired product of monosilane increases with increasing temperature. As such, a greater yield is expected in comparison with the previously discussed analogues. This arises from the direct relationship of the temperature of TCS disproportionation, increased rate of desorption of STC from the active sites, and ultimately, increased catalytic activity of the ligand.

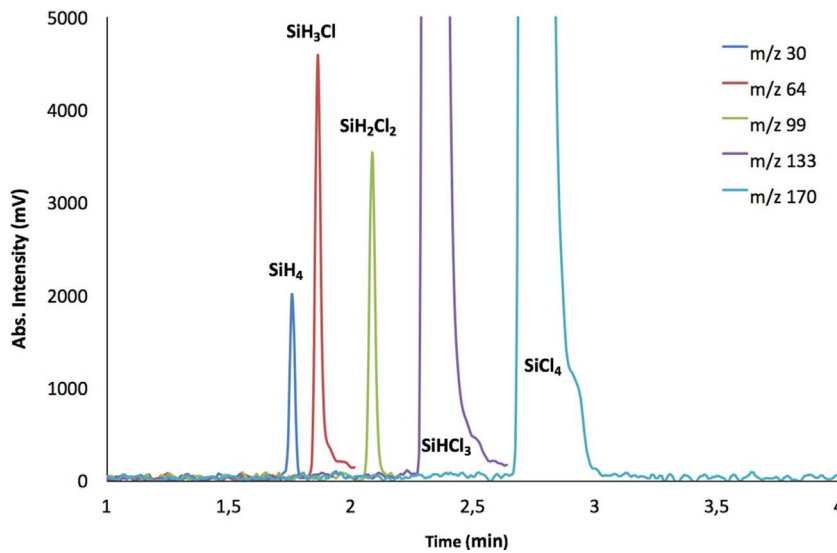


Fig. 4. Chromatogram of the sample mixture of chlorosilanes in SIM mode.

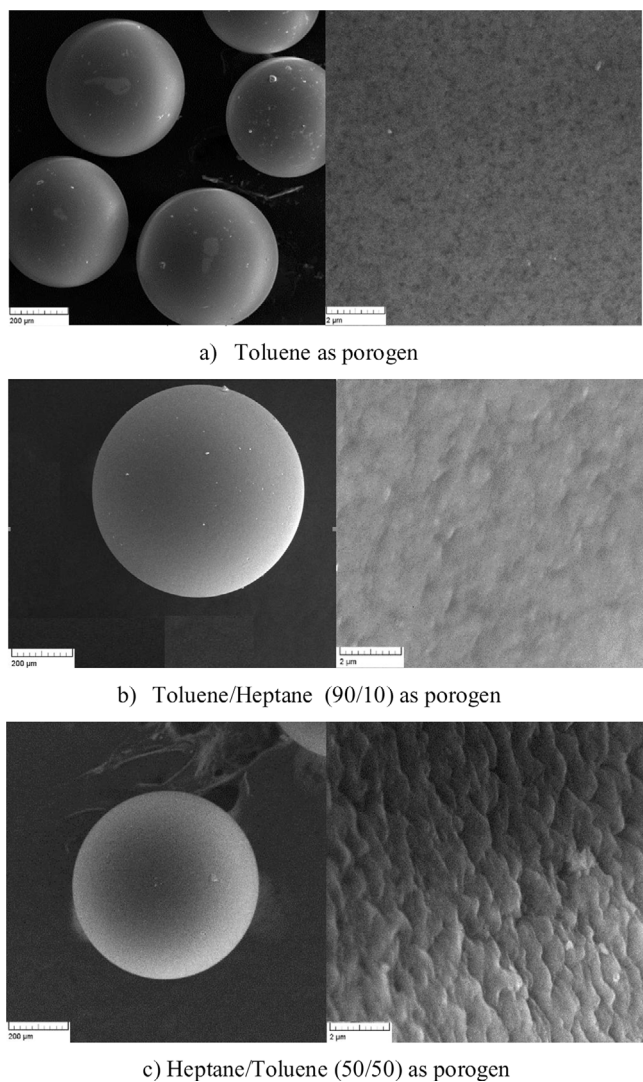


Fig. 5. SEM micrographs of the 2M5VP resins prepared using different porogens.

3.2. Comparison of catalytic activities

The catalytic activity of the resin under near equilibrium conditions was examined for the apparatus shown in Fig. 1. The reactor was loaded with the resins (2.35 cm^3 resins at 353 K), and the saturated vapor from the TCS bubbler was filled into reactor at a helium flow. Next, after one hour, the mixture of products in the reaction was injected into the GCMS to determine its composition. Sampling time was chosen experimentally (after one hour, the gas phase composition in the reactor is constant), the data are shown in Table 2.

The results indicate that the catalytic activity of 2M5VP-hep/tol is higher than those of 2M5VP-tol and 2M5VP-tol/hep and its conversion value at equilibrium was near quantitative (up to 99.8%). 2M5VP-tol and 2M5VP-tol/hep exhibited similar catalytic activities, therefore, to further study the kinetics of the disproportionation of TCS, resin 2M5VP-hep/tol was used.

3.3. Kinetics of the disproportionation of TCS

Since all resins have the same composition and differ only in structural characteristics, the most active resin was chosen for further experimental studies to obtain the kinetic dependence of the disproportionation of TCS.

Results of disproportionation of TCS for different temperatures for 2M5VP-hep/tol resin shown on the Fig. 9

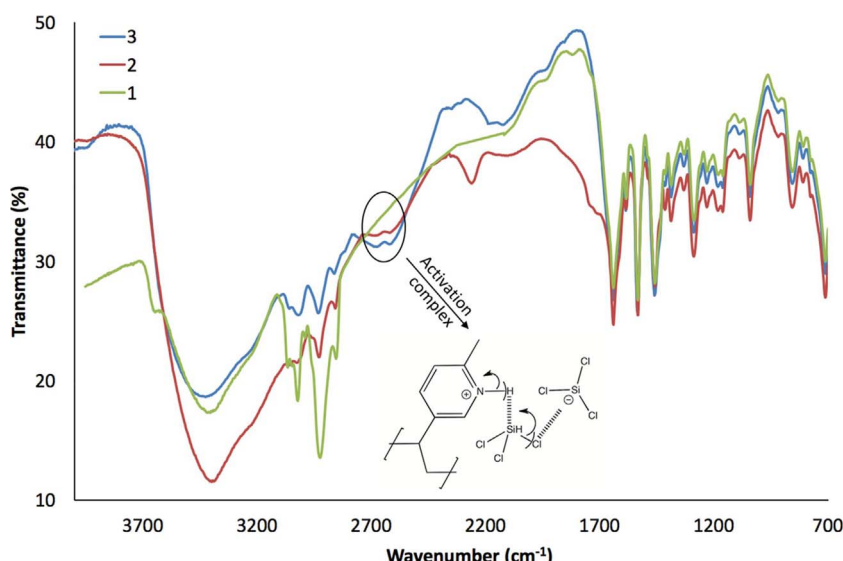
The effects of catalyst loading on the disproportionation of TCS were studied under 1.1 bar at 353 K. In Fig. 10, it is shown that the dependence of the TCS conversion from the residence time, obtained at three different catalyst loadings (2.35 cm^3 , 3.42 cm^3 and 4.82 cm^3). The residence time was changed to investigate the effect of catalyst loading on the conversion rate for the disproportionation of TCS. As can be seen, all points were placed on a common curve and indicates that for the same residence time at vastly different flow rates, the conversion of TCS is unchanged, i.e. the reaction proceeds in the kinetic region and diffusion is not a rate-limiting step.

Based on the ground, we have shown a logarithmic dependence of the reaction rate based on the concentration, which is described by the equation:

$$\ln V_o = (0.96 \pm 0.04) \ln C_{TCS} + (6.98 \pm 0.34), \quad (4)$$

where V_o – rate of the chemical reaction ($\text{mol l}^{-1} \text{ s}^{-1}$) and C_{TCS} – concentration of TCS (mol l^{-1}).

Fig. 6. FTIR spectra of 2M5VP-t resin before (1) and after interaction with TCS (2) and HCl (3).



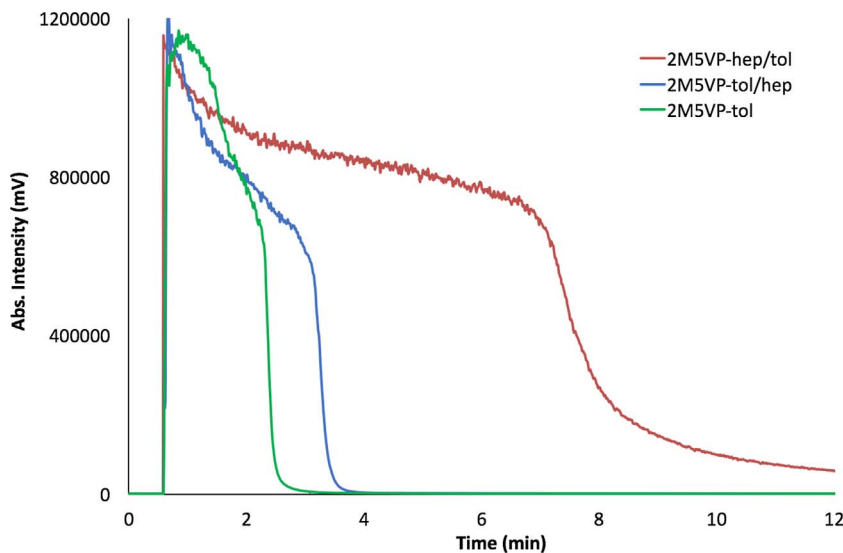


Fig. 7. Isotherm desorption of TCS from the different types of 2M5VP resins at 303 K.

From the slope of the plot, the reaction was found to be first order (0.96 ± 0.04). This indicates that the reaction rate depends on the concentration of TCS.

The presented experimental data were used to evaluate the rate constant as a function of temperature. The corresponding Arrhenius plot provided the expected linear curve (Fig. 11), and least squares fitting of the data yielded an equation for the temperature-dependent rate constant of reaction (1).

By processing the data by the least-squares method, we obtained an equation for determining the rate constant of the chemical reaction (5), (6):

$$\ln k = (0.31 \pm 0.01) - (2893.40 \pm 86.80) \cdot 10^3 / T, \quad (5)$$

$$\ln k = (2.68 \pm 0.08) - (4125.73 \pm 123.77) \cdot 10^3 / T, \quad (6)$$

From the slope of the Arrhenius plot (Fig. 11), the apparent activation energy of the process was determined to be: $E_a = 24.06 \pm 0.72 \text{ kJ mol}^{-1}$ for 2M5VP-hep/tol and $E_a = 34.30 \pm 1.03 \text{ kJ mol}^{-1}$ for Amberlyst A-21 resins.

To estimate the activation energy of SiCl_4 desorption at different temperatures, a classical technique was used by decomposing the

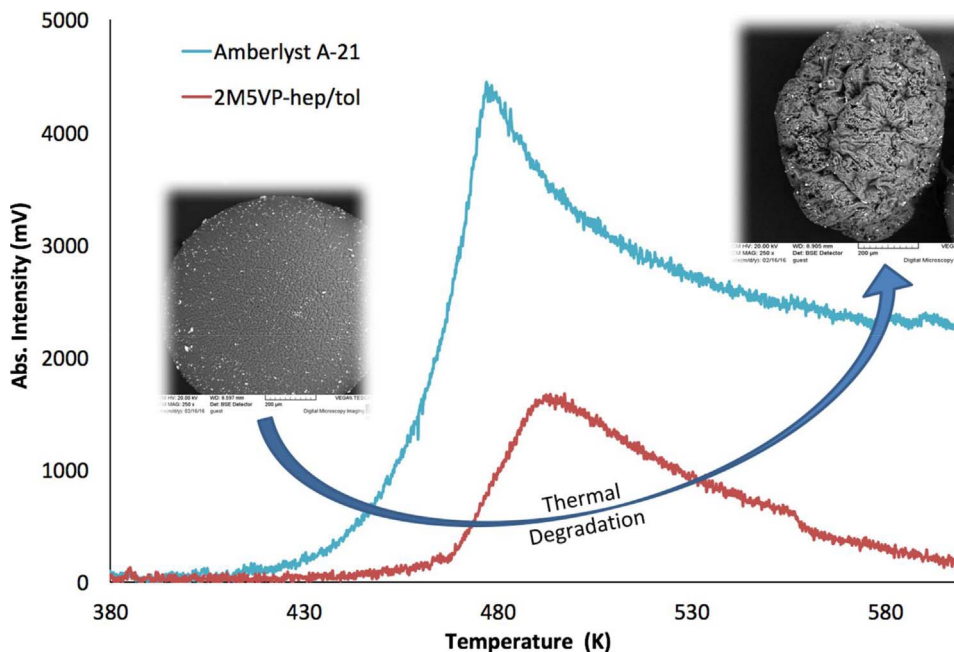


Fig. 8. Thermal stability 2M5VP vs. Amberlyst A-21 resins and SEM of the 2M5VP before and after thermal degradation.

Table 2

Concentration of the products of disproportionation of TCS for catalysts in near equilibrium conditions at 353 K.

Catalyst	Concentration, mol.% ^a				
	SiH_4	SiH_3Cl	SiH_2Cl_2	SiHCl_3	SiCl_4
Amberlyst A-21	3.5 ± 0.2	–	1.1 ± 0.1	4.1 ± 0.2	91.3 ± 4.6
2M5VP-tol	1.8 ± 0.1	–	3.3 ± 0.2	9.3 ± 0.5	85.6 ± 4.3
2M5VP-tol/hep	2.1 ± 0.2	–	2.7 ± 0.1	8.4 ± 0.4	86.8 ± 4.3
2M5VP-hep/tol	4.5 ± 0.2	–	–	0.2 ± 0.1	95.3 ± 48

^aRSD = 5%.

obtained spectra into the sum of the peaks described by Gauss distribution [64]. Based on the results of the TSD spectra (Fig. 12), we have calculated both the reaction order and activation energies of the desorption process and provided these data in Table 3. The dependences of TSD signals corresponding to ions of mass 133 (molecular ion of the silicon tetrachloride mass spectrum) are very similar and varied in intensity for different IER.

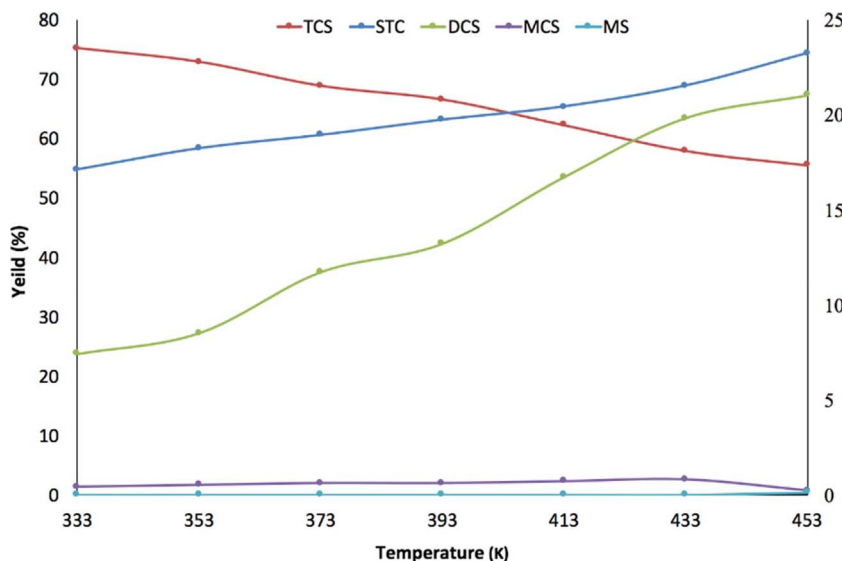


Fig. 9. Variable temperature disproportionation of TCS mediated by 2M5VP-hep/tol resin.

As can be seen in Fig. 12 and in Table 3, the maximum desorption temperatures indicate a low value of the binding energy of STC and the IER molecules.

In regard to the peaks of thermal desorption, it is worth noting that a significant difference in their forms was observed through the comparison of the high-temperature (HTA) and low-temperature areas (LTA) of the spectra. In the current samples, the ratio of LTA (τ) and HTA (δ) half-widths was equal to 1.68 (2M5VP-hep/tol) and 1.30 (Amberlyst A-21). The shape of the desorption peaks substantially depends on the desorption order and, consequently, can be used to unveil the order of desorption. A peak corresponding to the second order reactions has a symmetric shape ($\tau \approx \delta$), whereas a peak of the first order is asymmetric ($\tau > \delta$). The areas of the low- and high-temperature areas of the desorption peaks coincided (within RSD = 3%). This observation underscores the possibility of a first-order desorption.

Based on the values of δ and T_{\max} , the desorption activation energy E_d was calculated using the Redhead formula: [64]

$$E_d = \chi R T_{\max}^2 / \delta, \quad (7)$$

where χ – the order of the desorption (1 or 2 for the first and second order, respectively), T_{\max} – the temperature of the maximal TD signal, and δ – the half-width of the desorption peak at half-height.

The calculated activation energy of desorption E_d was 28.24 ± 0.84 kJ/mol for 2M5VP-hep/tol and 39.49 ± 1.18 kJ/mol for Amberlyst A-21. Therefore, the obtained desorption activation energy values pointed to the physical adsorption of silicon tetrachloride in all samples.

To determine the rate limiting step of TCS disproportionation, a non-stationary process was used. The dependence of the concentration distribution of the components of the mixture on the leading front of the flow of gas that passed through the reactor in its start-up period as shown in Fig. 13.

The concentration fronts of the components leave the reactor in a sequence corresponding to the growth of their molecular mass, i.e. when the process starts component redistribution along its length, to the process of the frontal chromatography, with the difference that in our case all the components of the mixture were subjected to a continuous chemical conversion. This explains the super-equilibrium yield of silane under non-stationary conditions in that the chemical equilibrium at the leading front of the flow of gas shifts toward the formation of silane due to the lagging of the fronts of heavy chlorosilanes.

Due to the low heat of adsorption and chemisorption of the silane on the active sites of the anion exchange resin, elution time of the front of the silane at the outlet of the reactor is virtually identical to the

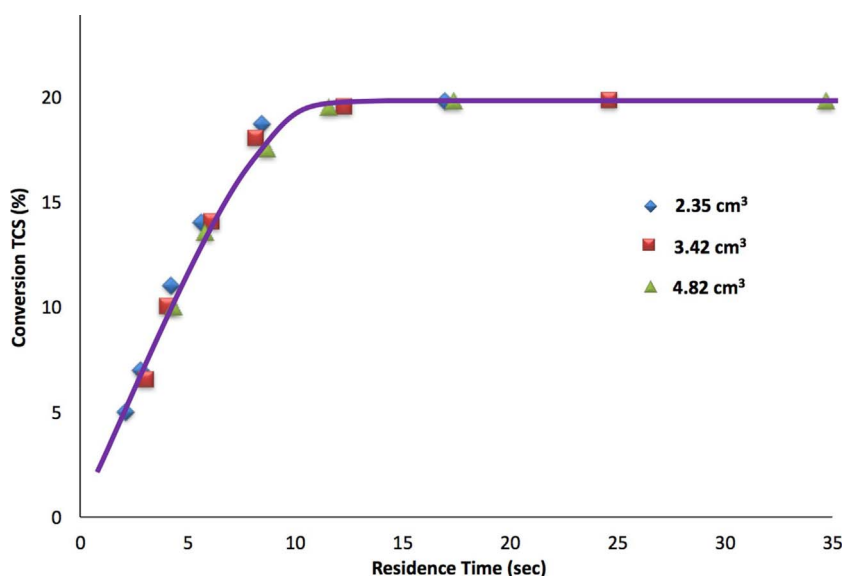


Fig. 10. Effect of catalyst loading on the conversion of TCS 2M5VP-hep/tol resin at 353 K.

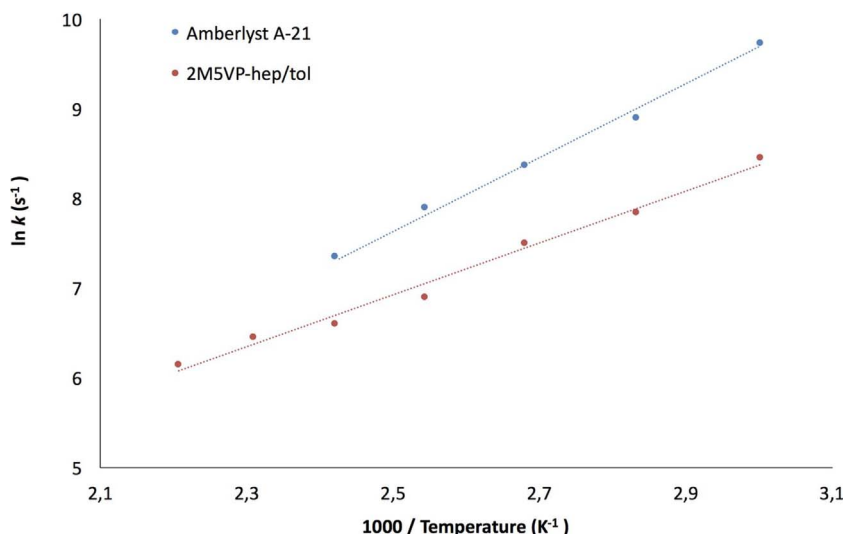


Fig. 11. Arrhenius plot of the reaction rate: the points represent the experimental data and the line represents the least squares fit (trend line).

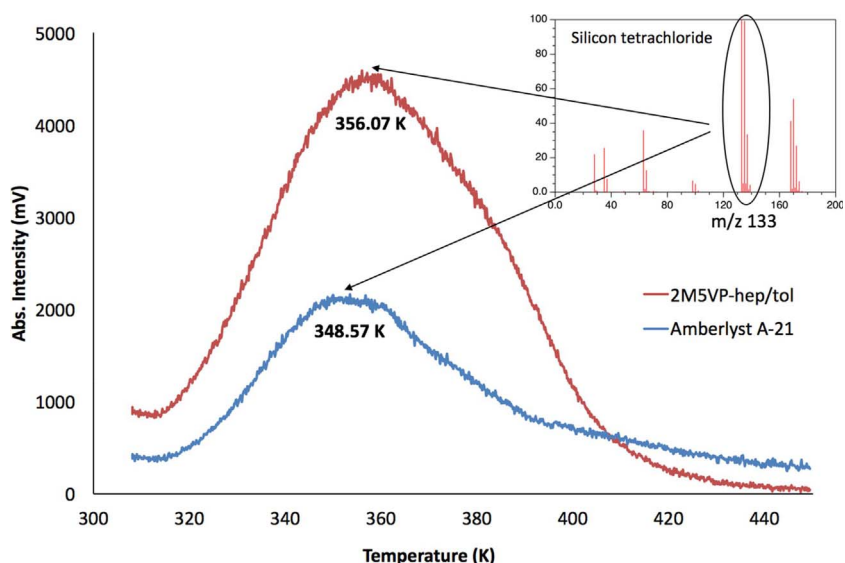


Fig. 12. The spectra of thermostimulated desorption (TSD) of SiCl_4 (SIM mode) from different resins.

Table 3
Desorption energy of SiCl_4 from IER.

IER	m/z	T_{\max} , K	τ LTA, K	δ HTA, K	χ	E_d , kJ/mol ^a
2M5VP-hep/tol	133	356.07	22.25	37.33	1	28.24
Amberlyst A-21	348.57	19.67	25.58	1	39.49	

^a RSD = 3%.

calculated time of appearance at the common flow front. This fact indicates a high rate of the stages of the sorption processes and disproportionation of chlorosilane molecules on the catalytic active sites. Thus, the only possibility for the limiting stage of the process is the desorption of STC molecules from the resin, forming relatively strong complexes with it [65].

To verify this assumption, the experiment was conducted under dynamic operation of the reactor during pulse feeding of TCS in the carrier gas. The diagram of the processes occurring in the reactor during pulsed feeding is shown in Fig. 14.

Fig. 14 shows that at the high frequency of pulses of TCS into the reactor, the STC formed in it does not have time to be removed by the carrier gas. As a result, a significant percentage of the active sites of the catalyst are temporarily deactivated by the adsorbed STC which causes a decrease in the catalytic activity. When the process temperature is

increased, the interval between the supply of TCS impulses required for the desorption of the STC decreases inversely with the change in temperature.

It should be noted that the organisation of the process of TCS disproportionation, according to the method described above, makes it possible to use it as a method for obtaining silane from TCS in a single step (through the realisation of a super-equilibrium yield of silane). Thus, it has been established that the limiting stage of the process of TCS disproportionation is the desorption of STC from the active sites of the catalyst.

As it was shown earlier, the limiting stage of the reaction is the desorption of STC from the active sites of the resin, thus inhibiting product formation. In the 2M5VP-hep/tol resin studied, the desorption of STC proceeds more easily than Amberlyst A-21, which is one of the reasons for greater catalytic activity.

3.4. Mechanism of disproportionation reaction of TCS

The mechanism of disproportionation of TCS on the resin has been previously proposed in Refs. [66,67]. First, the formation of the intermediate $\text{RNH}^+\text{SiCl}_3^-$ occurs along with further formation of an intermediate $[\text{RHSi}_2\text{HCl}_6]$, which subsequently breaks up into DCS and STC. Using FTIR analysis (Fig. 6), we have already established that the resin

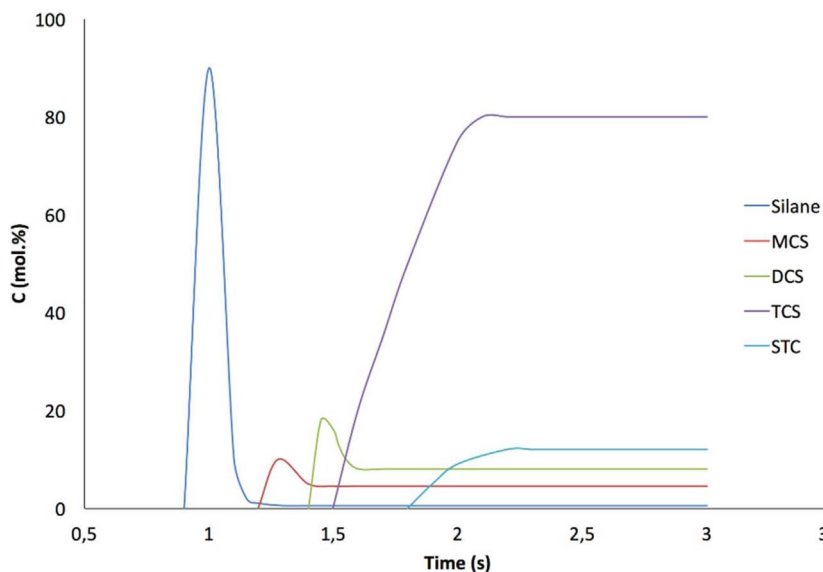


Fig. 13. Diagram showing distribution of chlorosilane concentrations at the outlet of the reactor in its start-up period.

undergoes protonation of the nitrogen atom in the pyridine ring after exposure HCl or TCS with concomitant formation of $\text{N}^+ \text{H} \cdots \text{Cl}^-$ (for HCl activation)/ $\text{N}^+ \text{H} \cdots \text{SiCl}_3^-$ (for STC activation).

At Fig. 15 presents the proposed mechanism of the disproportionation of TCS on the 2M5VP resin. At the first stage, the resin molecule is activated with TCS, which results in the formation of an ion pair H^+ and SiCl_3^- . In the second stage, a new molecule of TCS is coordinated near the ion pair, causing dissociation of the chlorine atom to form STC with the catalyst simultaneously stabilizing through the elimination of hydrogen to form DCS. In the third stage, a new molecule of TCS reactivates the resin molecule and the process repeats until the DCS formed as the MCS transforms into the silane, resulting in termination of the catalytic cycle and reactivation of the catalyst.

As the reaction is carried out in a continuous-flow reactor under dynamic conditions, cycle reproduction is not always possible due to the long desorption of STC from the active sites of the resin, as determined by EGA analysis, which explains the yield of DCS and MCS. Under dynamic conditions the low yield of silane differs from the thermodynamic calculations and data obtained in the equilibrium calculations.

Additionally, there are several of factors which may explain such a

low yield of silane, the most influential of these possible factors being dismutation.



Rather, it is likely that reactions (8)–(10) are operative which are also marked by the direct relationship of reaction rate and temperature.

The obtained catalyst from the point of view of the economic impact is more accessible in terms of cost compared to industrial Amberlyst A-21 resin, besides, the increase in the economic effect is due to the increased thermostability of the resulting catalytic system, which provides a higher yield of monosilane compared with analogues due to accelerated desorption of silicon tetrachloride from the active sites of the catalyst, which actually was established in the work.

The use of synthesized samples of 2M5VP resin has a greater economic potential, not only in terms of its physicochemical parameters, but also economic, an increase in the yield of monosilane by 0.5–1% leads to an economic benefit of 10–20%, when used in a reactive distillation apparatus.

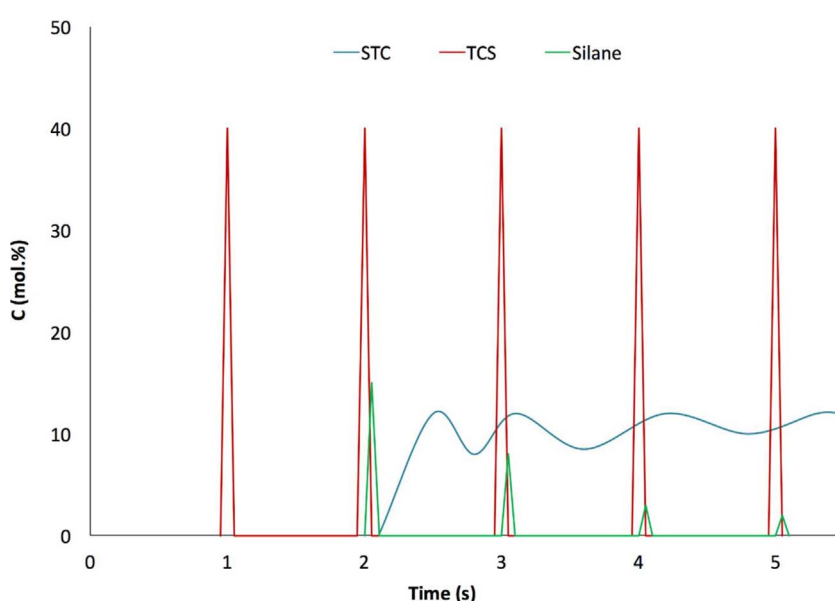


Fig. 14. Dynamic diagram of the operation of the reactor during pulse feeding of TCS in the carrier gas.



Fig. 15. Proposed catalytic mechanism of TCS disproportionation on the 2M5VP-hep/tol catalyst.

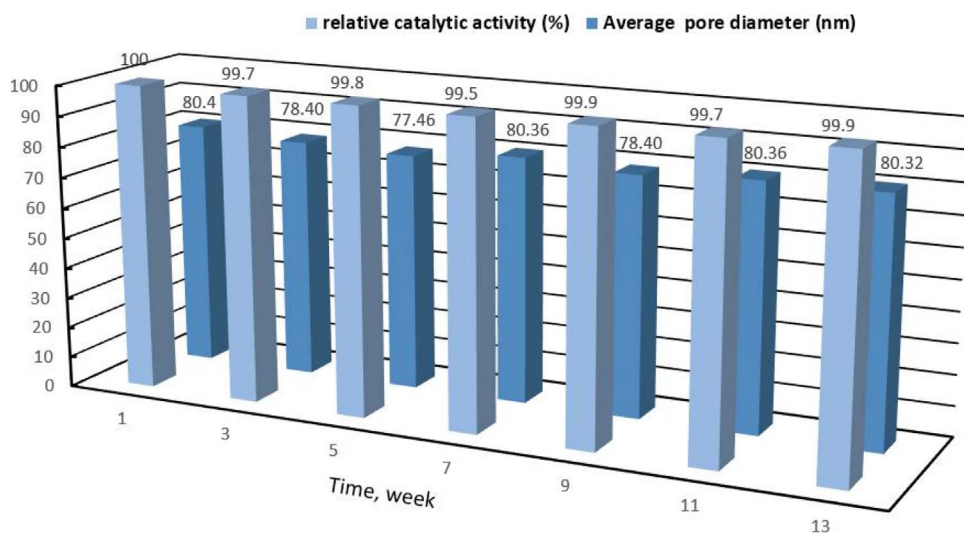
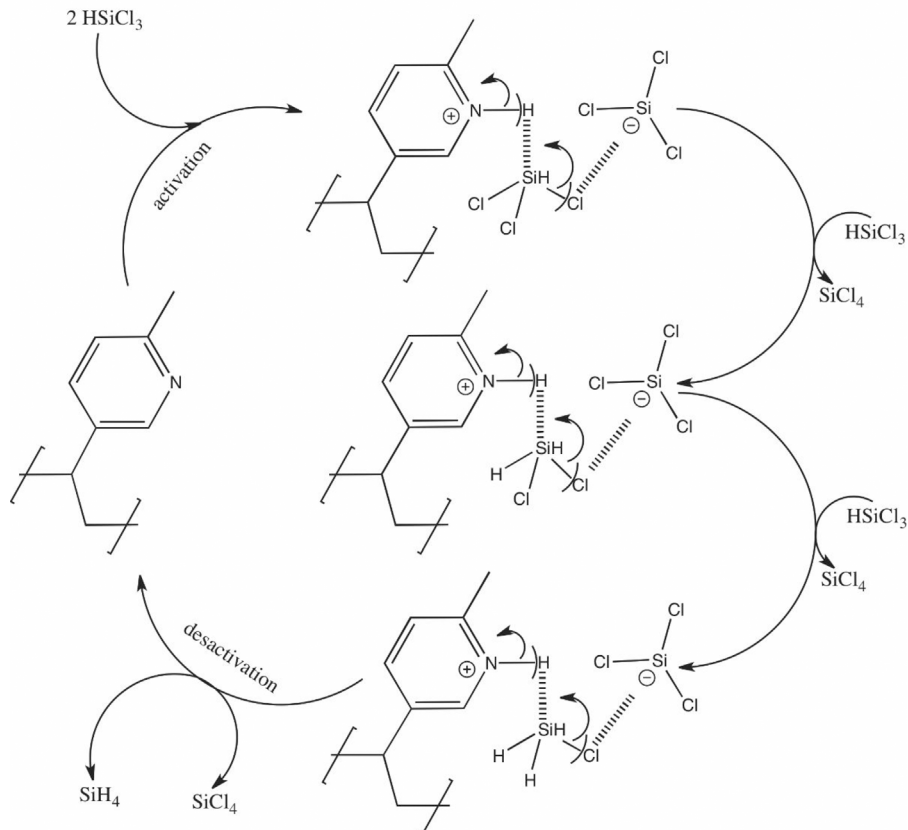


Fig. 16. Lifetime and deactivation of the catalyst 2M5VP-hep/tol in a part on relative catalytic activity and average pore diameter at 423 K in 13 weeks.

A study of the stability of the obtained 2M5VP-hep/tol samples also carried out at the temperature of 423 K with a carrier gas flow of 10 ml/min through the TCS on the change in catalytic activity and pore size for 13 weeks, the results are shown in Fig. 16. As can be seen from Fig. 16, the catalytic activity and the pore size of the resin vary within the instrument error, which indicates the stability of the 2M5VP-hep/tol sample for the selected time interval.

4. Conclusion

The work presented herein shows the development of a method of

disproportionation of trichlorosilane on an ion exchange resins based on 2-methyl-5-vinylpyridine and divinylbenzene as a catalyst. The catalyst was synthesized using suspension polymerization of 2M5VP/DVB with various composition diluents. In the synthesis of 2M5VP/DVB resins, three dilution degrees were adopted with the aim of producing different types of porous structures. The porous structure of the copolymer varies considerably depending on the applied porogen type and amount. A large proportion of the non-solvating agent, heptane, increases the pore diameter and decreases the specific surface area. In comparing the external surface and pore size of the prepared microspheres, it is noted that the microspheres synthesized with toluene/

heptane 50/50 as the porogen are more porous than those synthesized with toluene/heptane 90/10 or neat toluene.

Further, the temperature stability of the catalysts was determined using thermal desorption analysis and the results reveal that the samples are subjected to deactivation by thermodegradation via methyl chloride formation. However, compared to the industrial resin Amberlyst A-21 used in the disproportionation of TCS, the 2M5VP resin samples are more thermostable.

The catalytic activity of the resin under near equilibrium conditions was examined. The results indicate that the catalytic activity of 2M5VP-hep/tol is higher than that seen for 2M5VP-tol and 2M5VP-tol/hep and its conversion value at equilibrium was high up to 99.8%. To further study the kinetics of the disproportionation of TCS, 2M5VP-hep/tol was further studied. It was found that the reaction proceeds in the kinetic region and diffusion is not a rate-limiting step. From the slope of the corresponding plot, the order of reaction was found to be first order, indicating that the reaction order depends on the concentration of TCS. From the slope of the Arrhenius plot (Fig. 11), the apparent activation energy of the process was determined to be: $E_a = 24.06 \pm 0.72 \text{ kJ mol}^{-1}$ for 2M5VP-hep/tol and $E_a = 34.30 \pm 1.03 \text{ kJ mol}^{-1}$ for Amberlyst A-21 resins.

To determine the limiting stage of TCS disproportionation, a non-stationary reaction process and thermodesorption analysis of STC was performed. The calculated activation energy of desorption of STC was $28.24 \text{ kJ mol}^{-1}$ for 2M5VP-hep/tol and $39.49 \text{ kJ mol}^{-1}$ for Amberlyst A-21. The concentration fronts of the components leave the reactor in a sequence corresponding to the growth of their molecular mass, i.e. when the process starts redistribution component along its length, to the process of the frontal chromatography, with the difference that in our case, all the components of the mixture subjected to a continuous chemical conversion. This explains the super-equilibrium yield of silane under non-stationary conditions, the chemical equilibrium at the leading front of the flow of gas shifts toward the formation of silane due to the lagging of the fronts of heavy chlorosilanes. The limiting stage of the reaction is the desorption of STC from the active sites of the resin. In the 2M5VP-hep/tol resin prepared in this study, the desorption process of STC proceeds more easily than in Amberlyst A-21, thus explaining the higher observed catalytic activity, and its promise as a viable alternative to achieving TCS disproportionation.

Acknowledgments

The reported study was financially supported by Russian Foundation of Basic Research project No. 16-38-60192 mol_a_dk in part of synthesis IER, kinetic studies, project No. 15-48-02703 in part of GCMS analysis and The Ministry of Education and Sciences of the Russian Federation within the framework of the state task in the field of scientific activity (grant No. 11/17-01.10) in part of catalyst characterization within the framework of the Program of development of Flagship University of Russia for Nizhny Novgorod State Technical University n.a. R.E. Alekseev. Non-stationary method determine the limiting stage was supported by the Russian Science Foundation (grant No. 17-73-20275). Adsorption measurements was carried out on the equipment of the Collective Usage Center "New Materials and Resource-saving Technologies" (Lobachevsky State University of Nizhni Novgorod). Moreover authors are inordinately grateful to Dr. Rami Batrice from Georgetown University for his assistance in the improvement of the scientific style of manuscript.

Appendix A. Supplementary data

Supplementary data associated with this article can be found, in the online version, at <http://dx.doi.org/10.1016/j.apcatb.2017.10.062>.

References

- [1] S.H. Ahn, D.M. Chun, W.S. Chu, Int. J. Precis. Eng. Manuf. 14 (6) (2013) 873–874.
- [2] A.V. Shah, J. Meier, E. Vallat-Sauvain, et al., Sol. Energ. Mat. Sol. C 78 (1) (2003) 469–491.
- [3] Y. Nishi, R. Doering, *Handbook of Semiconductor Manufacturing Technology*, CRC Press, 2007 1720 p.
- [4] D.J. Eaglesham, M. Cerullo, Phys. Rev. Lett. 64 (1990) 1943–1947.
- [5] S. Chu, A. Majumdar, Nature 488 (7411) (2012) 294–303.
- [6] B.R. Bathey, M.C. Cretella, J. Mater. Sci. 17 (11) (2005) 3877–3896.
- [7] W.C. O'Mara, R.B. Herring, L.P. Hunt, *Handbook of Semiconductor Silicon Technology*, Noyes Publications, New Jersey, 1990 795 p.
- [8] M.A. Green, Sol. Energy 76 (1–3) (2004) 3–8.
- [9] M.J.-P. Duchemin, M.M. Bonnet, M.F. Koelsch, J. Electrochem. Soc. 125 (1978) 637–644.
- [10] A. Luque, S. Hegedus, *Handbook of Photovoltaic Science and Engineering*, John Wiley & Sons, 2011 (116 p.).
- [11] H.S.N. Setty, Carl L. Yaws, B.R. Martin, D.J. Wangler, Method of operating a quartz fluidized bed reactor for the production of silicon. U.S. Patent 3,963,838, 15 June 1976.
- [12] S.K. Iya, R.N. Flagella, F.S. Dipaolo, J. Electrochem. Soc. 129 (1982) 1531–1535.
- [13] S.M. Lord, R.J. Milligan, Method and apparatus for silicon deposition in a fluidized-bed reactor. PCT International Patent WO1996/041036, 3 April 1996.
- [14] K. Yasuda, T.H. Okabe, J. Jpn. Inst. Met. 74 (2010) 1–9.
- [15] Y.Q. Hou, G. Xie, Z.F. Nie, N. Li, Adv. Mater. Res. 881–883 (2014) 1805–1808.
- [16] S. Liu, W. Xiao, Chem. Eng. Sci. 127 (2015) 84–94.
- [17] Experimental Process System Development Unit for Producing Semiconductor Silicon Using Silane-to-Silicon Process/Union Carbide Corp Final Report, National Technical Information Center, Springfield, VA, 1981 DOE/JPL Contract 954334.
- [18] V.M. Vorotyntsev, Method for the production of silanes. RU 2152902, 20 July 2000.
- [19] M. Mehler, Electron. News 30 (1485) (1984) 54.
- [20] J.K. Iya, J. Cryst. Growth 75 (1986) 88–90.
- [21] V.M. Vorotyntsev, G.M. Mochalov, O.V. Nipruk, Russ. J. Appl. Chem. 74 (4) (2001) 621–625.
- [22] J. Harada, Process for production of silane. U.S. Patent 4,704,264, 3 November 1987.
- [23] K. Inoue, H. Miyagawa, M. Itoh, T. Abe, K. Koizumi, N. Yanagawa, Process for disproportionating silanes. U.S. Patent 4,667,048, 19 May 1987.
- [24] K.K. Seth, Chlorosilane disproportionation process. U.S. Patent 4,395,389, 26 July 1983.
- [25] C.J. Litteral, Disproportionation of chlorosilane. U.S. Patent 4,113,845, 12 Setember 1978.
- [26] L.L. Fadeev, The process for producing monosilane. RU 2077483, 20 April 2000.
- [27] A.V. Vorotyntsev, A.N. Petukhov, I.V. Vorotyntsev, T.S. Sazanova, M.M. Trubyanov, I.Y. Kopersak, E.N. Razov, V.M. Vorotyntsev, Appl. Catal. B 198 (2016) 334–346.
- [28] J.A. Rossi, R.K. Willardson, E.R. Weber, D.L. Rode, *Silicon epitaxy, Semiconductors and Semimetals*, Academic Press, 2001 p. 49.
- [29] D. Lynch, W. Ben, X. Ji, et al., TMS 2011 140th Annual Meeting and Exhibition, Materials Processing and Energy Materials, John Wiley, 2011, pp. 685–692.
- [30] R.A. Kornev, V.M. Vorotyntsev, A.N. Petukhov, E.N. Razov, L.A. Mochalov, M.M. Trubyanov, A.V. Vorotyntsev, RSC Adv. 6 (102) (2016) 99816–99824.
- [31] D.A. Mansfeld, A.V. Vodopyanov, S.V. Golubev, et al., Thin Solid Film 562 (2014) 114–117.
- [32] G. Bruno, P. Capezzuto, G. Cicala, F. Cramarossa, Plasma Chem. Plasma Proc. 6 (2) (1986) 109–125.
- [33] R. Platz, S. Wagner, Appl. Phys. Lett. 73 (1998) 1236–1238.
- [34] N. Ohse, K. Hamada, S.J. Kumar, et al., Thin Solid Films 516 (2008) 6585–6591.
- [35] L.A. Mochalov, R.A. Kornev, A.V. Nezhdanov, et al., Plasma Chem. Plasma Proc. 36 (3) (2016) 849–856.
- [36] C.E. Erickson, G.H. Wagner, Disproportion of silane derivatives. U.S. Patent 2,627,451, 3 February 1953.
- [37] R. Wagner, R. Maeker, H. Eversheim, H. Lange Method for preparing chlorosilane. U.S. Patent 2,005,011,359,2, 26 May 2005.
- [38] D.L. Bailey, Disproportionation of chlorosilanes. U.S. Patent 2,732,280, 24 January 1956.
- [39] D.L. Bailey, P.W. Shafer, G.H. Wagner, Wagner, G.H. Disproportion of chlorosilanes employing amine-type catalysts. U.S. Patent 2,834,648, 13 May 1958.
- [40] J.-K. Lepage, G. Soula, Preparation of silane from methyl dichlorosilane and chlorosilanes. U.S. Patent 4,605,543, 12 August 1986.
- [41] A.A. Zagorodni, *Ion Exchange Materials: Properties and Applications*, Elsevier, 2007, p. 477.
- [42] C.J. Bakay, Process for making silane. U.S. Patent 3,968,199, 6 July 1976.
- [43] L.M. Coleman, Process for the production of ultrahigh purity silane with recycle from separation columns. U.S. Patent 4,340,574, 20 July 1985.
- [44] S. Morimoto, Process for the disproportionation of chlorosilanes. U.S. Patent 4,613,489, 23 Setember 1986.
- [45] J.-K. Lepage, G. Soula, Process for the disproportionation of silanes. U.S. Patent 4,548,917, 22 October 1985.
- [46] C.J. Litteral, Process for preparing disproportionation products of chlorosilanes. DE Patent 2162537, 24 February 1977.
- [47] X. Huang, W.-J. Ding, J.-M. Yan, W.-D. Xia, Ind. Eng. Chem. Res. 52 (18) (2013) 6211–6220.
- [48] J.R. Alcántara-Avilá, H.A. Sillas-Delgado, J.G. Segovia-Hernández, et al., Comput. Chem. Eng. 78 (2015) 85–93.
- [49] V.M. Vorotyntsev, P.N. Drodzov, I.V. Vorotyntsev, S.N. Manokhina, S.S. Knysh, Pet. Chem. 53 (8) (2013) 627–631.
- [50] G.G. Devyatlykh, G.I. Panov, A.S. Kharitonov, J. Inorg. Chem. 32 (4) (1987) 1002–1005.
- [51] V.M. Vorotyntsev, V.V. Balabanov, D.A. Shamrakov, et al., High-Purity Subst. 3

(1987) 74–78.

[52] N.D. Grishnova, A.V. Gusev, A.N. Moiseev, G.M. Mochalov, N.V. Balanovskii, T.P. Kharina, Russ. J. App. Chem. 72 (10) (1999) 1761–1766.

[53] S. Brunauer, P.H. Emmet, E. Teller, J. Am. Chem. Soc. 60 (1938) 309.

[54] K.V. Otvagina, A.E. Mochalova, T.S. Sazanova, A.N. Petukhov, A.A. Moskvichev, A.V. Vorotyntsev, C.A.M. Afonso, I.V. Vorotyntsev, Membranes 6 (2) (2016) 31.

[55] ASTM-D1895, Apparent Density, Bulk Factor and Pourability of Plastic Materials. Annual Book of ASTM Standards, Part 35, Plastics General Test Methods, Nomenclature, ASTM, 1979, 2017.

[56] J. Lehto, R. Harjula, React. Funct. Polym. 27 (1995) 121.

[57] R. Kunin, Ion Exchange Polymers, Robert Krieger, New York, 1972, p. 340.

[58] V.M. Vorotyntsev, G.M. Mochalov, A.K. Matveev, A.V. Malyshev, I.V. Vorotyntsev, J. Anal. Chem. 58 (2) (2003) 156–159.

[59] C. Luiz, A. Alcino, N. Luciana, Mater. Lett. 58 (5) (2004) 563–568.

[60] F. Xin, F.M. Wang, H. Liao, S.F. Li, Chin. J. Chem. Eng. 8 (4) (2000) 287–293.

[61] L. Li, J. Cheng, X. Wen, P. Pi, Z. Yang, Chin. J. Chem. Eng. 14 (4) (2006) 471–477.

[62] S.C. Bernstein, J. Am. Chem. Soc. 92 (3) (1970) 699–700.

[63] W.-J. Ding, J.-M. Yan, W.-D. Xiao, Ind. Eng. Chem. Res. 53 (27) (2014) 10943–10953.

[64] D.P. Woodruff, T.A. Delchar, Modern Techniques of Surface Science, Cambridge Univ Press, Cambridge, 1994 568 p.

[65] I.I. Lapidis, L.A. Niselson, Tetrachlorosilane and trichlorosilane/M, Chemistry (1970) 109–115.

[66] M.A. Ring, R.L. Jenkins, R. Zanganeh, H.C. Brown, J. Am. Chem. Soc. 93 (1) (1971) 265–267.

[67] K.A. Chulpanov, K.H. Rakhmatullayev, T. Dzhalilov, Polym. Sci. 27 (4) (1985) 804–807.